

Power System Stabilizers Layout via Flower Pollination Algorithm

E. S. ALI

Electrical Department, Faculty of Engineering, Jazan University,
Jazan, KINGDOM OF SAUDI ARABIA

Abstract:- In this article, the optimum layout of Power System Stabilizers (PSSs) using Flower Pollination Algorithm (FPA) is developed in a multimachine environment. The PSSs values tuning problem is turned into an optimization task which is treated by FPA. FPA is used to check for optimum controller parameters by reducing an eigenvalues based objective function involving the damping factor, and the damping ratio of the lightly damped modes. The implementation of the developed FPA based PSSs (FPAPSS) is compared with Particle Swarm Optimization (PSO) based PSSs (PSOPSS) and the Conventional PSSs (CPSS) for various loading conditions and disturbances. The results of the developed FPAPSS are confirmed via time domain analysis, eigenvalues and some indices. Also, the results are introduced to prove the effectiveness of the developed algorithm over the PSO and conventional one.

Key-Words: Power System Stabilizers; Flower Pollination Algorithm; Particle Swarm Optimization; Power System Stability.

Received: November 22, 2021. Revised: October 21, 2022. Accepted: November 23, 2022. Published: December 31, 2022.

1. Introduction

Power system stability is one of the modern considerable issues in the analysis of power systems, [1]. One of the forcible instances of this is an interconnected power system. The loaded long tie-lines could account for a diversity of stability issues, [2]. This directs to the divergence of the ultimate investigators towards designing a suitable PSS. Recently, numerous research missions are based on an area named "Heuristics from Nature" in which the analogies of social systems are being exercised, [3]. These approaches when used in the research community can demonstrate their susceptibility of finding optimum solutions of non-differentiable, multi-model, and compound objective functions. Numerous new approaches have been applied for designing a PSS as Differential Evolution (DE), [4], PSO, [5], Bacterial Swarm Optimization (BSO), [6], Harmony Algorithm (HA), [7], Bacteria Foraging (BF) [8], Bat Algorithm (BA) [9], Water Cycle Algorithm (WCA), [10], Backtracking Search Algorithm (BSA), [11], Grey Wolf Algorithm (GWA), [12], Whale Optimization Approach (WOA) [13], Cuckoo Search Algorithm (CSA), [14], [15], Genetic Algorithm (GA), [16], and Kidney-Inspired Algorithm (KIA), [17]. All of these approaches are based upon Artificial Intelligence (AI). A novel optimization algorithm called FPA has been addressed by Yang, [18]. It is created by the fertilization process of flowering plants, [19], [20]. It has only one parameter p (switch probability), that makes the algorithm easier to apply and quicker to link an optimum solution. The transferring switch among local and global fertilization can sponsor escaping from the local

lower solution. Moreover, it examines its efficacy in another problem as in [21]. Also, it is serene from the inspection that the purpose of the FPA to settle the problem of PSS design has not been illustrated. This supports the utility of the FPA to cure this problem.

2. Problem Formulation

2.1 Power System Paradigm

The complex nonlinear paradigm related to n units connected power system, can be constituted by a set of differential equations as:

$$X = f(X, U) \quad (1)$$

where X is the vector of the state elements and U is the vector of input variables.

$X = [\delta, \omega, E'_q, E_{fd}, V_f]^T$ and U is the product signals of PSSs in this article. δ and ω are the rotor angle and speed, respectively. Also, E'_q, E_{fd} and V_f are the inner, the field, and excitation voltages respectively.

The linearized models around a point are exercised in the design of PSS. Thus, the state equation of a power system with m PSSs can be constituted as:

$$X = AX + BU \quad (2)$$

where A is a matrix of $5n \times 5n$ and equals $\partial f / \partial X$ while B is a matrix of $5n \times m$ and equals $\partial f / \partial U$. Both A and B are evaluated at a certain operating point. X is a vector of $5n \times 1$ and U is a $m \times 1$ input vector.

2.2 PSS Structure

Power system companies recognize CPSS structure due to the readiness of online settings and the lack of affirmation of the stability related to some variable structure techniques. Otherwise, a universal analysis of the effects of distinct CPSS parameters on the overall dynamic performance of the power system is illustrated in [1, 2]. It is clear that the adequate election of the CPSS parameters leads to satisfying performance pending the system disturbances. The structure of the i^{th} PSS is presented by:

$$\Delta U_i = K_i \frac{ST_W}{(1+ST_W)} \left[\frac{(1+ST_{1i})(1+ST_{3i})}{(1+ST_{2i})(1+ST_{4i})} \right] \Delta \omega_i \quad (3)$$

This structure involves a gain, washout filter, a dynamic compensator and a limiter as it is displayed in Fig. 1. The product signal is a supplementary input signal, ΔU_i to the organizer of the excitation system. The input signal $\Delta \omega_i$ is the change in speed from the synchronous one. The stabilizer gain K_i is utilised to locate the value of damping to be injected. Then, a washout filter makes it just act as a contra oscillator in the input signal to evade steady state error in the terminal voltage. Moreover, two lead-lag circuits are involved to exclude any delay among the excitation and the electric torque. The limiter is included to prohibit the product signal of the PSS from driving the excitation system into heavy saturation [2].

In this article, the value of the washout time constant T_W is fixed at 10 second, the values of time constants T_{2i} and T_{4i} are kept at 0.05 second. The gain K_i and time constants T_{1i} , and T_{3i} are determined via FPA.

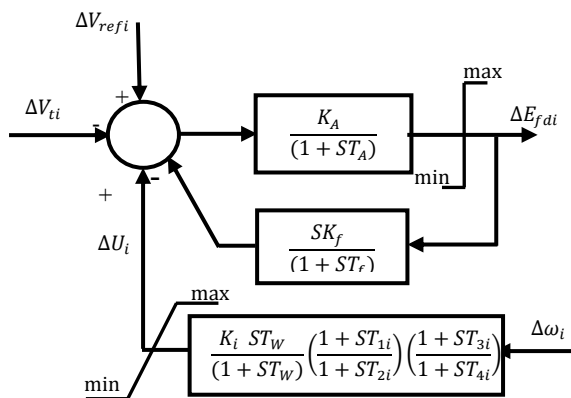


Fig. 1. Block diagram of i^{th} CPSS with excitation system.

2.3 Test System

A multimachine system involves three units and nine buses. The system data and loading events are mentioned in [2, 8].

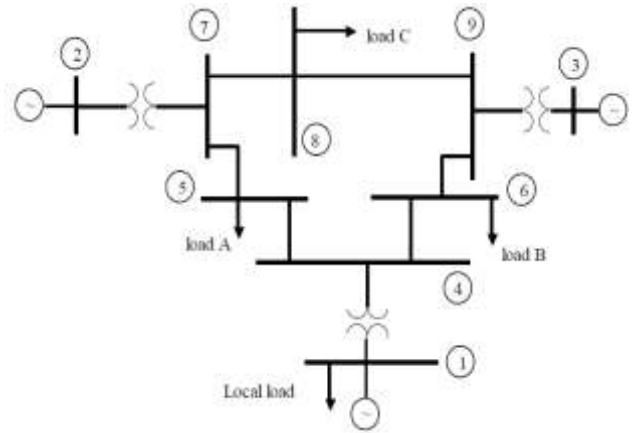


Fig. 2. Multimachine test system.

3. Overview of FPA

FPA was introduced by Yang in 2012 [18]. It is inspired by the fertilization process of flowers. Real-world design problems in engineering are multiobjective [19, 20]. These objectives conflict with one another. FPA has been adopted to resolve PSS design problems.

3.1. Characteristics of Flower Pollination

The main purpose of a flower is reproduction via fertilization. Flower fertilization is correlating with the transfer of pollen, which is often associated with pollinators. Some flowers and bees have a very specialized flower-pollinator sharing [18]. Fertilization can be terminated by self or cross-fertilization. Also, insects and birds may follow Lévy flight behavior in which they journey distance steps obeying a Lévy distribution. In addition, flower constancy acts as an incremental step employing the similarity of two flowers [19, 20]. The objective of flower fertilization is the survival of the fittest and the optimum reproduction of plants. This can be treated as an optimization task of plant species. All of these factors created optimum reproduction of the flowering plants.

3.2. Flower Pollination Algorithm

For FPA, the following four steps are used:
 Step 1: Global fertilization represented in biotic and cross-fertilization processes, as pollen-carrying pollinators fly following Lévy flight [20].

Step 2: Local fertilization represented in a biotic and self-fertilization as the process does not require any pollinators.

Step 3: Flower constancy which can be expanded by insects, which is on a par with a reproduction probability that is identical to the identity of two flowers involved.

Step 4: The interactivity of local and global pollination is planned by $p \in [0, 1]$, slightly biased toward local pollination.

The former steps have to be modified to conveniently updating equations. For example at the global pollination step, the pollinators load the flower pollen gametes, so the pollen can journey over an extended distance. Consequently, global pollination and flower constancy step can be designated by:

$$x_i^{t+1} = x_i^t + \gamma L(\lambda)(g_* - x_i^t) \quad (4)$$

Where x_i^t is the pollen i , and g_* is the present best solution found between all solutions at the present iteration. Here γ is a scaling factor controlling the step size.

In fact, $L(\lambda)$ the Lévy flights are based on step size that corresponds to the intensity of the pollination. Since long distances can be covered by insects using diverse distance steps, a Lévy flight can be utilized to simulate this behaviour. That is, $L > 0$ from a Lévy distribution.

$$L \sim \frac{\lambda \Gamma(\lambda) \sin(\pi\lambda / 2)}{\pi} \frac{1}{s^{1+\lambda}} \quad (s > s_0 > 0) \quad (5)$$

$\Gamma(\lambda)$ is the standard gamma function, and this distribution is valid for large steps $s > 0$.

For the local fertilization, both Step 2 and Step 3 can be represented as

$$x_i^{t+1} = x_i^t + \varepsilon(x_j^t - x_k^t) \quad (6)$$

where x_j^t and x_k^t are pollen from distinct flowers of the same plant species mimicking the flower constancy in a limited neighborhood. For a local random walk, x_j^t and x_k^t comes from the same species then ε is drawn from a uniform distribution as $[0, 1]$.

The flowchart of FPA is presented in Fig. 3. The data of FPA is displayed in the appendix.

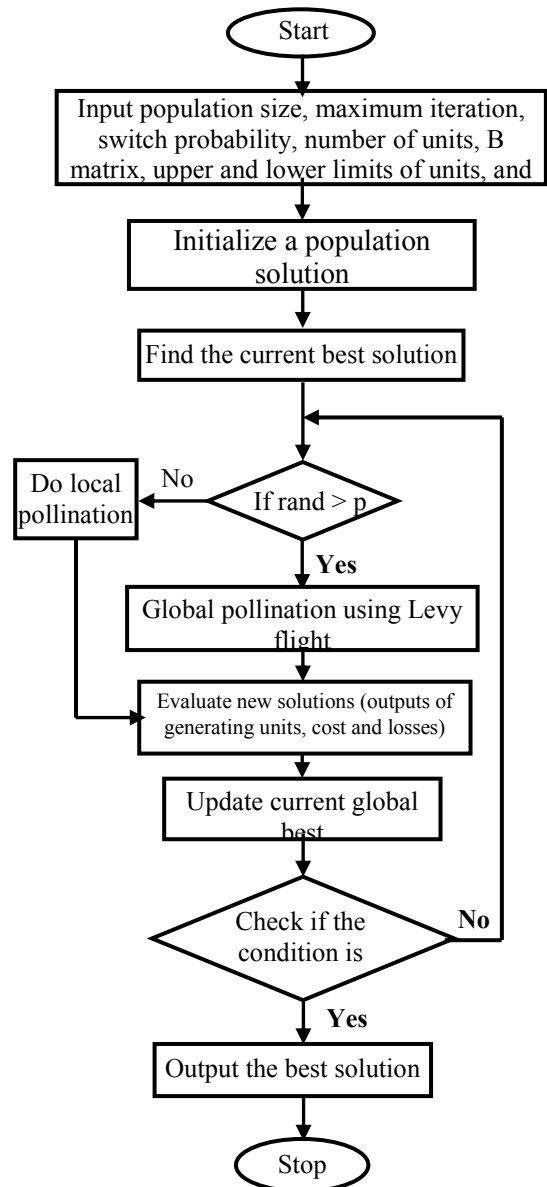


Fig. 3. Flowchart of FPA.

4. Objective Function

For a multimachine power system the objective function is modified to include the interaction between machines. The parameters of the PSS may be selected to minimize the following objective function:

$$J_t = \sum_{j=1}^{np} \sum_{\sigma_{ij} \geq \sigma_0} (\sigma_0 - \sigma_{ij})^2 + \sum_{j=1}^{np} \sum_{\xi_{ij} \geq \xi_0} (\xi_0 - \xi_{ij})^2 \quad (7)$$

This will place the system closed loop eigenvalues in the D-shape sector characterized by $\sigma_{ij} \leq \sigma_0$ and

$\xi_{ij} > \xi_0$ as shown in Fig. 4.

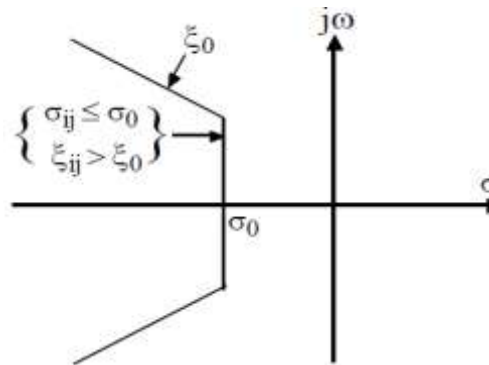


Fig. 4. D-shaped sector in the negative half of the plane.

In this article, σ_0 and ξ_0 are picked to be -0.5 and 0.1 respectively. Typical limits of the optimized values are [1-100] for K and [0.06-1.0] for T_{1i} and T_{3i} . Optimization process based on the objective function J can be formed as: lower J according to:

$$\begin{aligned} K_i^{min} &\leq K_i \leq K_i^{max} \\ T_{1i}^{min} &\leq T_{1i} \leq T_{1i}^{max} \\ T_{3i}^{min} &\leq T_{3i} \leq T_{3i}^{max} \end{aligned} \quad (8)$$

This article focuses on optimum tuning of PSSs using FPA. The target of the optimization is to reduce the objective function to enhance the system behaviour in terms of settling time and overshoots under distinct loading conditions and then designing a small order controller for easy application.

5. Results and Simulations

In this section, the sublimity of the developed FPA algorithm in designing PSS compared with optimized PSS with PSO and CPSS is illustrated. The eigenvalues and their damping ratios for distinct operating conditions and controllers are displayed in Table 1. Also, the controller parameters are obtained in Table 2.

Table (1) Mechanical modes and ζ for distinct loading events and algorithms.

	FPAPSS	PSOPSS	CPSS
Light load	-1.23±0.64j,0.89	-0.62±0.87j, 0.58	-0.19±0.69j,0.26
	-6.27±6.18j, 0.71	-2.16±3.91j, 0.48	-2.35±4.15j, 0.48
	-3.05±5.62j,0.48	-3.05±7.41j,0.38	-3.24±5.2j,0.52
Normal load	-1.27±0.79j,0.85	-0.74±0.92j,0.62	-0.24±0.75j,0.3
	-6.02±6.35j,0.69	-2.23±4.07j,0.48	-2.41±4.42j,0.47
	-3.11±5.15j,0.52	-3.64±8.17j,0.41	-3.32±5.34j,0.52
Heavy load	-1.08±0.86j,0.78	-0.71±0.79j,0.69	-0.33±0.89j,0.34
	-7.07±5.02j,0.82	-1.58±3.72j,0.39	-1.96±4.32j,0.41
	-4.23±7.44j,0.49	-3.28±8.01j,0.38	-3.09±5.25j,0.5

Table (2) Values of controllers for distinct algorithms.

	FPAPSS	PSOPSS	CPSS
PSS ₁	K=40.7381	K=29.4632	K=14.4386
	T ₁ =0.6326	T ₁ =0.4224	T ₁ =0.2652
	T ₃ =0.4738	T ₃ =0.6795	T ₃ =0.8952
PSS ₂	K=9.4541	K=7.5429	K=5.1659
	T ₁ =0.4673	T ₁ =0.6541	T ₁ =0.5242
	T ₃ =0.1851	T ₃ =0.3441	T ₃ =0.2032
PSS ₃	K=6.4623	K=7.2855	K=8.3287
	T ₁ =0.4324	T ₁ =0.6358	T ₁ =0.5817
	T ₃ =0.1971	T ₃ =0.3759	T ₃ =0.4268

5.1 Response under normal load condition

The validation of the behavior under distinct disturbance is affirmed by applying a 20% increase of mechanical torque of unit-1. Figs.5-7, display the response of $\Delta\omega_{23}$, $\Delta\omega_{13}$ and $\Delta\omega_{12}$ due to this disturbance under normal loading condition. It can be noted that the system with the developed FPAPSS is more stabilized than PSOPSS and CPSS. In addition, the needed average settling time to alleviate system oscillations is approximately 1.1 second with FPAPSS, 1.86 second for PSOPSS, and 8.35 second with CPSS so the developed controller is competent for provisioning proper damping to the low frequency oscillations.

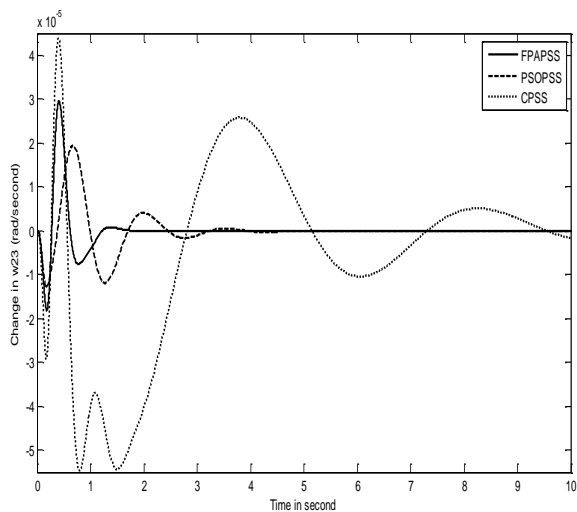


Fig. 5. Change in $\Delta\omega_{23}$ for normal load.

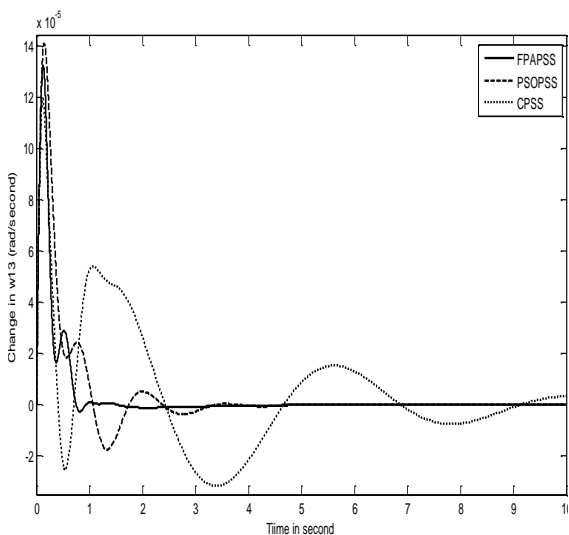


Fig. 6. Change in $\Delta\omega_{13}$ for normal load.

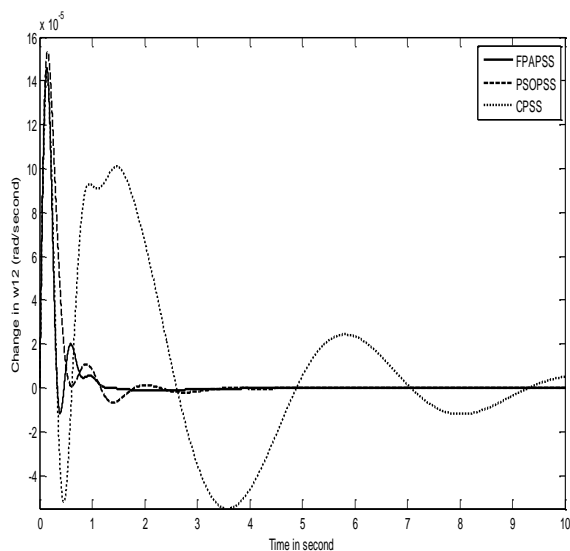


Fig. 7. Change in $\Delta\omega_{12}$ for normal load.

5.2 Response under light load condition

Figs. 8-10, show the response of the system under light loading conditions with fixing the parameters of the controller. It is clear that the developed FPAPSS has good alleviation characteristics to system modes and stabilizes rapidly the system. Also, the average settling time of oscillations are $T_s = 1.12, 1.78,$ and 8.32 seconds for FPAPSS, PSOPSS, and CPSS respectively. Hence, the developed FPAPSS outlasts effectively PSOPSS and CPSS in minifying oscillations and attenuating settling time. Consequently, the developed FPAPSS expands the limit of power system stability.

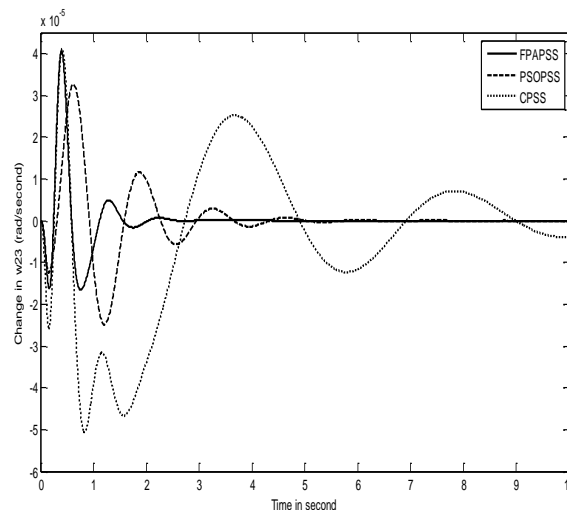


Fig. 8. Change in $\Delta\omega_{23}$ for light load.

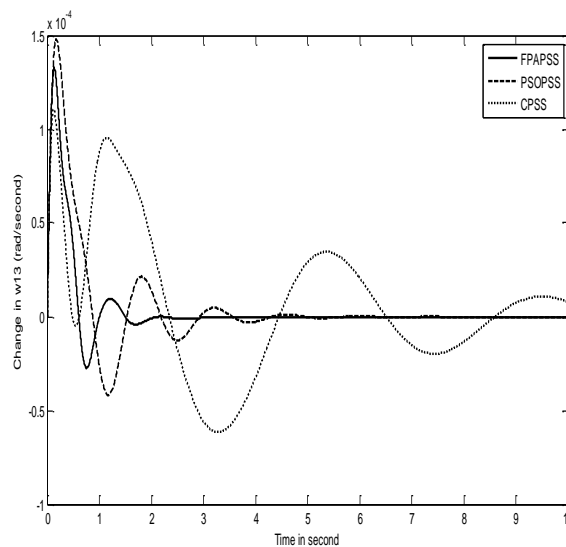


Fig. 9. Change in $\Delta\omega_{13}$ for light load.

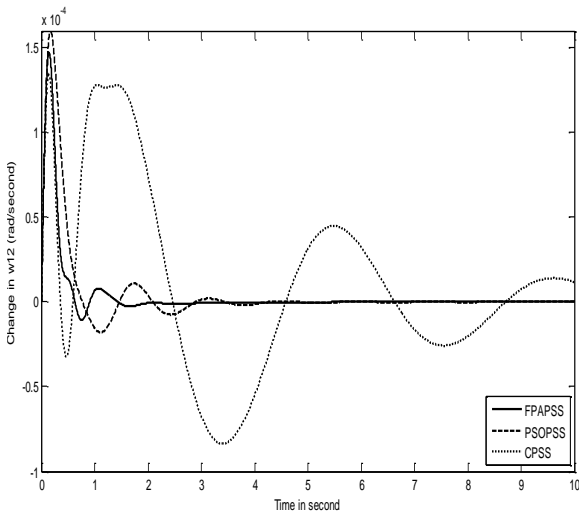


Fig. 10. Change in $\Delta\omega_{12}$ for light load.

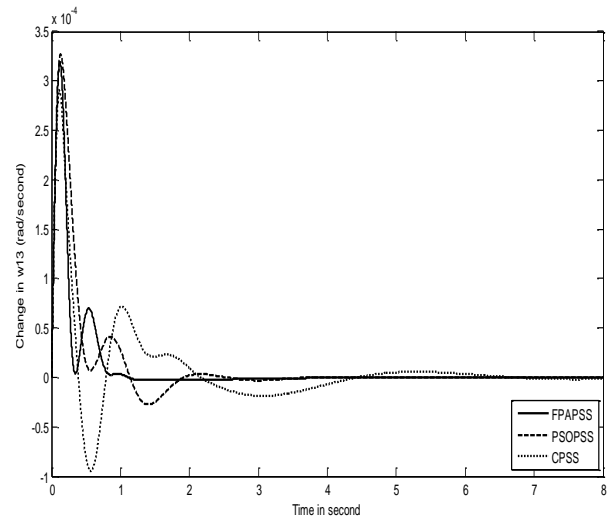


Fig. 12. Change in $\Delta\omega_{13}$ for heavy load.

5.3 Response under heavy load condition

Figs. 11-13, show the response of the system under heavy loading conditions. These figures point to the supremacy of the FPAPSS in lowering the settling time and suppressing system oscillations. Also, the average settling time of these oscillations are $T_s = 0.96, 1.26,$ and 3.76 seconds for FPAPSS, PSOPSS, and CPSS respectively. Hence, FPAPSS controller enhances greatly the alleviation characteristics of power system.

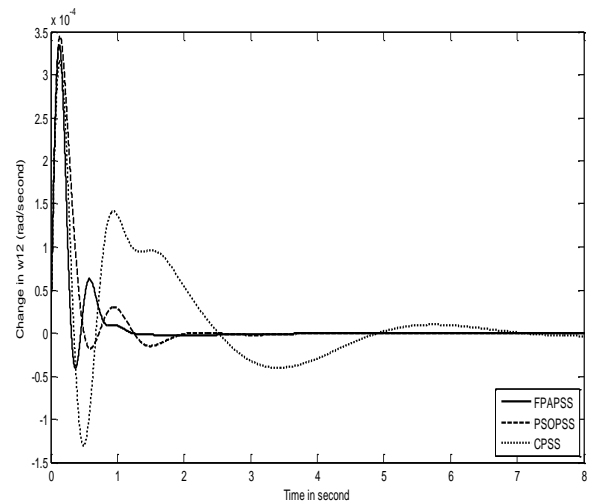


Fig. 13. Change in $\Delta\omega_{12}$ for heavy load.

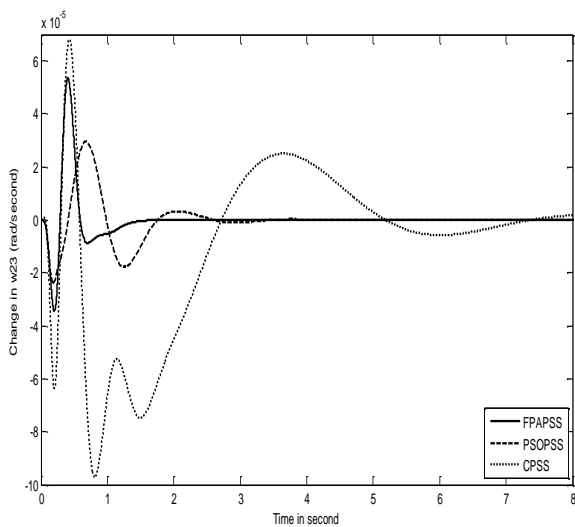


Fig. 11. Change in $\Delta\omega_{23}$ for heavy load.

5.4 Performance indices

To estimate the superiority of the developed FPAPSS, several performance indices: the Integral of Absolute value of the Error (IAE), and the Integral of Time multiply Absolute value of the Error (ITAE) are written as:

$$IAE = \int_0^{20} (|\Delta w_{12}| + |\Delta w_{23}| + |\Delta w_{13}|) dt$$

(9)

$$ITAE = \int_0^{20} t (|\Delta w_{12}| + |\Delta w_{23}| + |\Delta w_{13}|) dt$$

(10)

The weaker the account of indices have, the higher the system response is. Numerical results of performance indices for distinct events are recorded in Table (3). It is manifest that the values of these indices with the FPAPSS are junior compared with those of PSOPSS and CPSS. This believes that the speed deviations of all units, settling time, and overshoot, are constricted extremely by setting the developed FPA based tuned PSSs.

Table (3) Performance indices for distinct algorithms.

	IAE * 10 ⁻⁴			ITAE * 10 ⁻⁴		
	CPSS	PSO PSS	FPA PSS	CPSS	PSO PSS	FPA PSS
Light event	7.21	0.2663	0.0445	23.74	0.4642	0.2734
Normal event	15.87	0.3973	0.0654	34.05	0.7756	0.5978
Heavy event	24.79	0.5686	0.100	45.89	0.9729	0.8387

6. Conclusion

FPA is presented in this article for optimum designing of PSSs parameters. The PSSs parameters tuning problem is converted as an optimization problem and FPA is employed to search for optimum parameters. An eigenvalue based objective function reflecting the combination of damping factor and damping ratio is optimized for distinct operating conditions. Simulation results evidence the superiority of the developed FPAPSS in assigning good damping behaviour to system oscillations for distinct loading events. Also, the developed FPAPSS affirms its efficacy than PSOPSS and CPSS through some indices. Coordination of PSS and FACT devices via FPA is the future field of this work.

Appendix

Parameters of FPA: Maximum number of iterations = 500, population size = 20, probability switch = 0.8.

References

[1] P. Kundur, "Power System Stability and Control", McGraw-Hill, 1994.
 [2] P. M. Anderson and A. A. Fouad, "Power System Control and Stability", Wiley-IEEE Press, 2nd edition, 2002.
 [3] X. Yang, "Engineering Optimization: An Introduction with Metaheuristics Applications", Wiley, 2010.

[4] Z. Wang, C. Y. Chung, K. P. Wong, and C. T. Tse, "Robust Power System Stabilizer Design under Multi-Operating Conditions Using Differential Evolution", IET Generation, Transmission & Distribution, Vol. 2, No. 5, 2008, pp. 690-700.
 [5] H. Shayeghi, H. A. Shayanfar, A. Safari, and R. Aghmasheh, "A Robust PSSs Design Using PSO in a Multimachine Environment", Int. J. of Energy Conversion and Management, Vol. 51, No. 4, 2010, pp. 696-702.
 [6] S. Abd-Elazim, and E. Ali, "A Hybrid Particle Swarm Optimization and Bacterial Foraging for Optimal Power System Stabilizers Design", Int. J. of Electrical Power and Energy Systems, Vol. 46, No. 1, March 2013, pp. 334-341.
 [7] K. A. Hameed, and S. Palani, "Robust Design of Power System Stabilizer Using Harmony Search Algorithm", ATKAFF, Vol. 55, No. 2, 2014, pp. 162-169.
 [8] E. Ali, and S. M. Abd-Elazim, "Power System Stability Enhancement via Bacteria Foraging Optimization Algorithm", Int. Arabian Journal for Science and Engineering, Vol. 38, No. 3, March 2013, pp. 599-611.
 [9] E. Ali, "Optimization of Power System Stabilizers Using BAT Search Algorithm", Int. J. of Electrical Power and Energy Systems, Vol. 61, No. C, Oct. 2014, pp. 683-690.
 [10] N. Ghaffarzadeh, "Water Cycle Algorithm Based Power System Stabilizer Robust Design for Power Systems", J. of Electrical Engineering, Vol. 66, No. 2, 2015, pp. 91-96.
 [11] M. Shafiullah, M. A. Abido, and L. S. Coelho, "Design of Robust PSS in Multimachine Power Systems Using Backtracking Search Algorithm", In Proceedings of the 18th Int. Conf. on Intelligent System Application to Power Systems (ISAP), Sep. 2015, pp.1-6.
 [12] M. R. Shakarami, I. F. Davoudkhani, "Wide-Area Power System Stabilizer Design based on Grey Wolf Optimization Algorithm Considering The Time Delay", Electric Power Systems Research, Vol. 133, April 2016, pp. 149-159.
 [13] N. A. M. Kamari, I. Musirin, Z. Othman, and S. A. Halim "PSS Based Angle Stability Improvement Using Whale Optimization Approach", Indonesian J. of Electrical Engineering and Computer Science, Vol. 8, No. 2, Nov. 2017, pp. 382 -390.
 [14] S. Abd-Elazim, and E. Ali, "Optimal Power System Stabilizers Design via Cuckoo Search Algorithm", Int. J. of Electrical Power and Energy Systems, Vol. 75 C, Feb. 2016, pp. 99-107.

- [15] D. Chitara, K. R. Niazi, A. Swarnkar, and N. Gupta, “*Cuckoo Search Optimization Algorithm for Designing of a Multimachine Power System Stabilizer*”, IEEE Transactions on Industry Applications, Vol. 54, No. 4, 2018, pp. 3056 - 3065.
- [16] M. Shafiullah, M. J. Rana, M. S. Alam, and M. A. Abido, “*Online Tuning of Power System Stabilizer Employing Genetic Programming for Stability Enhancement*”, J. of Electrical Systems and Information Technology, Vol. 5, 2018, pp. 287-299.
- [17] S. Ekinici, A. Demiroren, and B. Hekimoglu, “*Parameter Optimization of Power System Stabilizers via Kidney-Inspired Algorithm*”, Trans. Inst. Meas. Control, Vol. 41, No. 5, 2019, pp. 1405-1417.
- [18] X. S. Yang, M. Karamanoglu, X. He, “*Multi-Objective Flower Algorithm for Optimization*”, Procedia Comput Sci, 2013, Vol. 18, pp.61-68.
- [19] B. J. Glover, “*Understanding Flowers and Flowering: An Integrated Approach*”, Oxford, UK: Oxford University Press; 2007.
- [20] X. S. Yang, “*Engineering Optimization: an Introduction with Metaheuristics Applications*”, Wiley, 2010.
- [21] A. Abd-Elaziz, E. Ali and S. M. Abd-Elazim, “*Flower Pollination Algorithm for Optimal Capacitor Placement and Sizing in Distribution Systems*”, Electric Power Components and System, Vol. 44, Issue 5, 2016, pp. 544-555.

Creative Commons Attribution License 4.0 (Attribution 4.0 International, CC BY 4.0)

This article is published under the terms of the Creative Commons Attribution License 4.0

https://creativecommons.org/licenses/by/4.0/deed.en_US